

Synthesis and spectroscopic characterization of multifunctional D- π -A benzimidazole derivatives as potential pH sensors

Anja Beč¹, Robert Vianello^{2*} and Marijana Hranjec^{1*}

¹Department of Organic Chemistry, Faculty of Chemical Engineering and Technology,
University of Zagreb, Croatia

²Laboratory for the Computational Design and Synthesis of Functional Materials, Division of
Organic Chemistry and Biochemistry, Ruđer Bošković Institute, Zagreb, Croatia

*Corresponding authors: Prof. Marijana Hranjec (e-mail: mhranjec@fkit.hr), Dr. Robert Vianello (e-mail: robert.vianello@irb.hr)

Abstract: We report multifunctional D- π -A molecular systems having the *N,N*-diethylamino group as a pH sensitive donor unit connected to the electron accepting substituents such as the cyano moiety and the pH responsive benzimidazole fragment. For that purpose we have synthesized three types of derivatives, namely acrylonitrile, Schiff base and iminocoumarin derived benzimidazoles, whose photophysical characterization has been carried out in several polar and non-polar organic solvents as well as aqueous solution buffers with different pH. Computationally supported determination of species involved in prototropic equilibria, including their respective p*K*_a values, has been performed to aid in understanding structural and substituent effects on their UV–Vis and fluorescence spectral properties and pH sensing potentials. Both sets of results jointly indicate that all molecules are predominantly unionized under neutral conditions, while their transition towards monocationic forms, responsible for spectroscopic response changes, occurs at pH \approx 1–4 for acrylonitriles **4–5**, pH \approx 4–5 for Schiff bases **11–12**, and pH \approx 4.5–6.5 for iminocoumarins **7–8**, thus increasing their practical attractiveness for a broad range of applications in the same order.

Keywords: acrylonitriles, benzimidazoles, DFT computational analysis, iminocoumarins, pH sensors, Schiff bases, spectroscopic characterization

Introduction

Heterocyclic molecular systems with prominent and diverse spectral features and responses are among the most extensively studied classes of organic compounds. Design and development of small molecules for (chemo)sensing and optoelectronic applications is of great interest in organic chemistry and sensing technology.^{1,2}

The fact that the benzimidazole nuclei shares a structural similarity with naturally occurring purines promoted its applications in molecular biology and medicinal chemistry.^{3,4} The benzimidazole moiety can serve as a multifunctional unit and an especially attractive building block in D- π -A systems, thus allowing different applications in optoelectronics, as functional materials and as pH sensors.^{1,5} The photophysical and chemical properties of push-pull systems are defined by the position, number, electron donating and accepting strengths of donor and acceptor groups, and their chemical nature.^{1,6-8} Since benzimidazole has electron accepting and π -bridging properties that can be combined with its chromogenic pH sensitivity, switching and metal-ion chelating properties, it became an unavoidable building block for the design and synthesis of heteroaromatic derivatives possessing different applications in optoelectronics⁹ and as non-linear optics (NLO), in photovoltaics,^{10, 11} for sensing and bioimaging^{12,13} *etc.* D- π -A heteroaromatic systems are usually tailored to have an electron donating group placed opposite to the electron withdrawing group on the conjugated organic skeleton, with the possibility to manipulate the fluorescent response and signaling recognition processes. Since benzimidazole has a multifunctional nature with desirable photophysical properties as well as potentially selective binding sites for different analytes, it is very often incorporated in such D- π -A structures.^{1,14}

Naturally occurring and synthetic coumarin derivatives display diverse biological activities and are important structural motifs in medicinal chemistry, but have also attracted much attention as important fluorescent optical compounds with a broad applicability in a wide range of different applications.^{15,16} Thus, iminocoumarins are described as functional and optical materials,¹⁷ fluorescent brighteners,¹⁸ laser dyes,¹⁹ solar energy collectors,²⁰ pigments and probes for physiological measurements in living systems,²¹ charge-transfer agents²² or fluorescent labels.²³ Suchlike derivatives possess good solubility and interesting photochemical characteristics while their spectral responses can be further modified upon substituting the iminocoumarin skeleton on various positions, mostly with electron-donating groups at position 7 along with electron-accepting groups at position 3.²⁴ The photophysical properties can be modulated by introducing a longer π -electronic conjugation, as for example, in several benzo- and benzazole-derived coumarins.^{25,26}

Schiff bases, as one of the most extensively studied compounds, play an important role in electron donor- π -electron acceptor molecular systems (D- π -A systems) based on charge-transfer interactions due to their excellent properties as chromophores and fluorophores.²⁷ Besides their broad spectrum of biological activities, they are also considered as catalysts in synthesis,²⁸ chemodosimeters,²⁹ corrosion inhibitors,³⁰ fluorescent probes for imaging,^{31,32} colorimetric indicators,³³ and as optical chemical sensors.³⁴ Considering Schiff bases as pH sensors in aqueous solutions is typically challenging, since the complex protonation and tautomeric equilibria are involved together with the sensitivity of the imino bond towards the hydrolysis in polar solvents. Schiff bases derived mostly from a variety of heterocyclic rings are most frequently described as optical chemical sensors.^{35,36}

Furthermore, the cyano group, is a strong electron acceptor in D- π -A systems capable to impact the spectral characteristics of the characterized molecules, as well as the basicity of the neighboring sites and their corresponding pK_a values.³⁷ Ideal intermediates for affording substituted nitriles are acrylonitriles, a nitrile structure attached to a vinylic moiety.³⁸ This functional group has the potential to establish hydrogen bonds, hydrophobic interactions, and it is a key factor in the creation of supramolecular interactions.³⁹

Based on presented considerations, herein we present multifunctional D- π -A molecular systems containing the *N,N*-diethylamino group on a phenyl ring as a pH sensitive donor group connected via a linker (imino bond, acrylonitrile group and coumarin nuclei) to the pH sensitive benzimidazole moiety (Fig. 1). The photophysical characterisation and computationally supported determination of species involved in prototropic equilibria, including their matching pK_a values, have been performed in order to better understand the effects of the D- π -A molecular structure and the type of the linker on the UV-Vis spectral properties, and pH sensing potential of these chromophores.

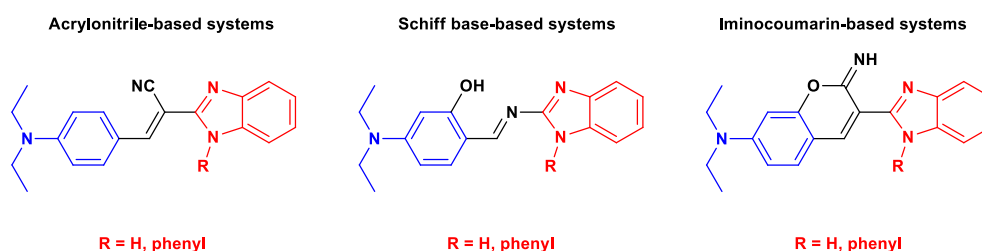
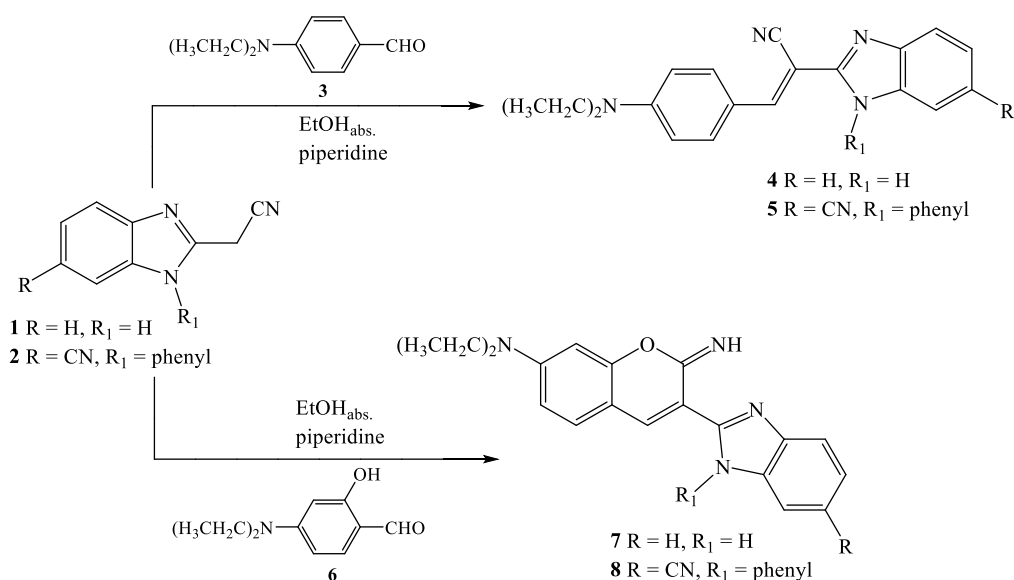


Figure 1. Structures of investigated benzimidazole derivatives.

2. Results and Discussion

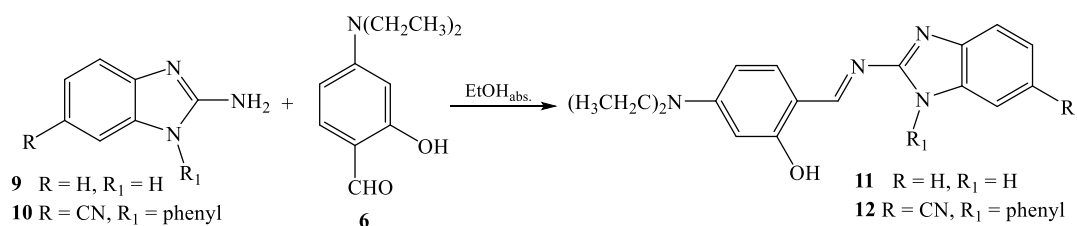
2.1. Chemistry

Benzimidazoles **4-5**, **7-8** and **11-12** were prepared according to the two experimental procedures presented in Schemes 1 and 2. For the synthesis of targeted acrylonitriles and iminocoumarins, the main synthetic intermediates 2-cyanomethylbenzimidazoles **1-2** and 2-aminobenzimidazoles **9-10** were afforded according to the previously published experimental procedure. Within the condensation with 4-*N,N*-diethyl-aminobenzaldehyde **3** in slightly basic media, acrylonitriles **4** and **5** were obtained in moderate reaction yields. Due to the cyclocondensation with 4-*N,N*-diethylamino-2-hydroxybenzaldehyde **6** in ethanol and piperidine, iminocoumarins **7** and **8** were prepared.



Scheme 1. Synthesis of acrylonitrile **4-5** and iminocoumarin derivatives **7-8**.

Targeted benzimidazole derived Schiff bases obtained in the reaction of 2-amino-benzimidazoles **9-10** with 4-*N,N*-diethylamino-2-hydroxybenzaldehyde **6** in ethanol.



Scheme 2. Synthesis of Schiff bases **11-12**.

The structures of all prepared benzimidazoles were confirmed by ^1H and ^{13}C NMR spectra and elemental analysis. The structural analysis was performed based on the chemical shifts in both ^1H and ^{13}C NMR spectra, and on the H–H coupling constants values in the ^1H spectra. Appearance of the singlet related to the acrylonitrile proton around 8.0 ppm confirmed the formation of acrylonitrile derived benzimidazoles **4-5**. The formation of targeted Schiff bases **11-12** was confirmed by the observation of a singlet related to the proton of the imino group in the ^1H NMR spectra as well as a signal for the C atom of the imino group in the ^{13}C NMR spectra.

2.2. Spectroscopic characterization

Basic photophysical properties of the prepared derivatives were characterised by UV-Vis spectra recorded in several organic solvents of different polarities with the chromophore solution concentration of 1×10^{-5} mol dm $^{-3}$. The main focus was to study the influence of the linker type between the *para*-*N,N*-dimethylamino group placed as a pH sensitive donor group on the phenyl ring and the benzimidazole skeleton, as well as the type of the substituent placed on the benzimidazole nitrogen on spectroscopic characteristics.

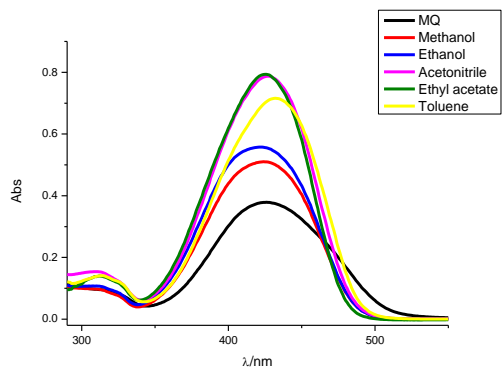
2.2.1. UV-Vis absorption spectra

In order to evaluate the impact of the solvent polarity on the spectroscopic features of studied benzimidazole compounds, stock solutions were prepared in six organic solvents. Absorption spectra were recorded at the same concentration at room temperature in the same range. For the spectroscopic characterization, solvents of a high purity grade with different $E_T(30)$ polarity parameters were used. The absorption spectra of representative studied derivatives were presented in Fig. 2, for other studied compounds in Supporting Material (Fig. S1). Electronic absorption and emission data for studied compounds are presented in Table 1.

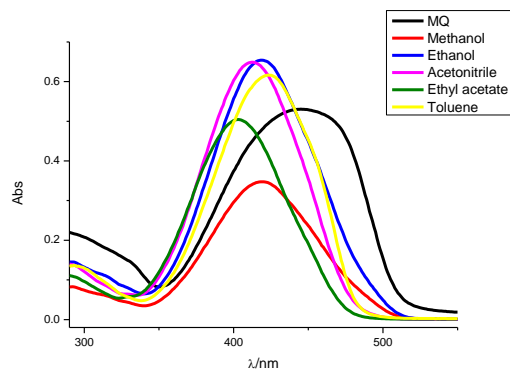
The absorption spectra of compounds **4**, **5**, **8** and **11** show one main absorption band which are centered for compound **4** around 425 nm, for **5** around 410 nm, for **8** ranging from 405 nm to 445 nm, and for **11** from 415 to 425 nm. In most used solvents, compounds **7** and **12** showed two main absorption bands. When considering the absorption spectra of the *N*-unsubstituted acrylonitrile derivative **4**, the most intensive absorbance with a slight blue shift in comparison to toluene and MQ water, was observed in acetonitrile and ethyl acetate, while in toluene the absorption spectra showed the increase of intensity. The lowest absorption intensity has been observed in hydrogen donating solvents, MQ water, methanol and ethanol in comparison to other solvents. Iminocoumarin **8** substituted with cyano and phenyl group, displayed the highest absorbance intensity in ethanol and acetonitrile with significant decrease

of intensity in methanol. In MQ water we might observe the red shift of absorption maxima, opposite in comparison to ethyl acetate.

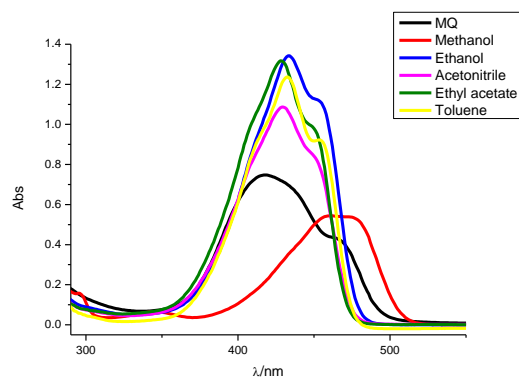
a) Compound **4**



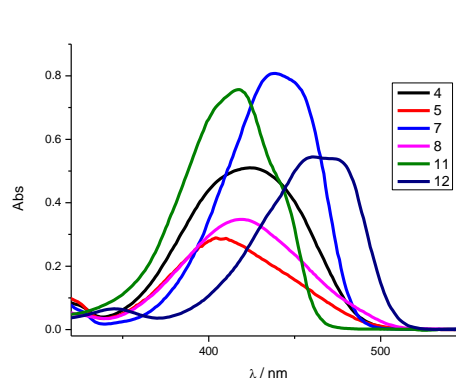
b) Compound **8**



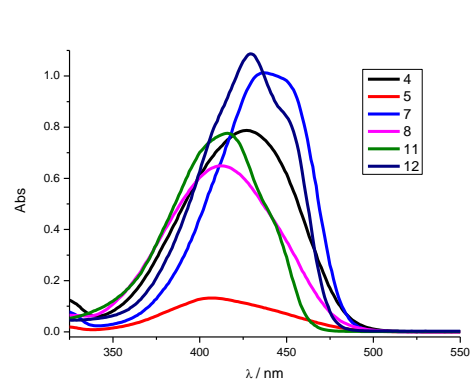
c) Compound **12**



d) All compounds in methanol



e) All compounds in acetonitrile



f) All compounds in toluene

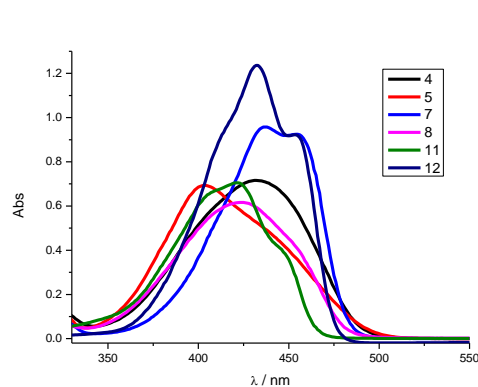


Figure 2. UV-Vis spectra of **4** (a), **8** (b) and **12** (c) at concentration 2×10^{-5} mol dm⁻³ in organic solvents of varying polarities; compared absorption spectra of all studied compounds in methanol (d), acetonitrile (e), and toluene (f).

N-phenyl substituted Schiff base with the cyano group placed at the benzimidazole nuclei **12**, showed the highest intensity in ethanol, while in methanol we observed the most significant hypochromic effect as well as significant red shift of maxima for ~30 nm in comparison to other solvents. In nonpolar aprotic toluene, **12** showed slight blue shift and also decrease of absorbance intensity. Considering all absorption spectra taken in methanol, the highest intensity has been observed for unsubstituted iminocoumarin **7**, while the lowest intensity has been observed for *N*-phenyl and cyano substituted acrylonitrile **5** together with the blue shift of absorption maxima. The most significant red shift of absorption maxima has been observed for *N*-phenyl and cyano substituted Schiff base **12**. Compound **12** showed in acetonitrile the increase of intensity with two absorption bands at 429 and 452 nm, while all other studied compounds showed one main band. The significantly lowest intensity as well as blue shift of absorption maxima has been observed for *N*-phenyl and cyano substituted acrylonitrile **5**, while iminocoumarin **7** showed red shift of absorption maxima in comparison to other studied compounds. In toluene, the lowest intensity has been displayed by *N*-phenyl and cyano substituted iminocoumarin **8**, while *N*-phenyl and cyano substituted acrylonitrile **5** showed the most significant blue shift of maxima. *N*-phenyl and cyano substituted Schiff base **12** showed the highest absorption intensity. Compounds **4**, **7** and **11** showed two absorption bands.

2.2.2. Fluorescence emission spectra

Fluorescence emission spectra were recorded at lower concentrations, namely 1×10^{-6} mol dm⁻³ for **10** and **13–15**, and 2×10^{-7} mol dm⁻³ for **11–12** due to differences in their solubilities. The emission spectra were recorded in several solvents using excitation wavelengths determined from the absorbance maxima, and were uncorrected for the inner filter effects. The emission spectra of representative iminocoumarines **7** and **8** are shown in Figure 3, while in Figure S17 for other systems that did not exhibit significant fluorescence intensity. Electronic absorption and emission data for studied compounds are presented in Table 1.

Emission spectra of **7** and **8** indicated one emission band and one maximum in all solvents as well as the strong impact of the solvent polarity on the fluorescence characteristics. In the most polar water solution, both compounds showed hypochromic shift of the fluorescence intensity, while **7** showed significant decrease of fluorescence intensity with slight bathochromic shift of emission maxima. By decreasing the solvent polarity, **7** exerted the hyperchromic effect.

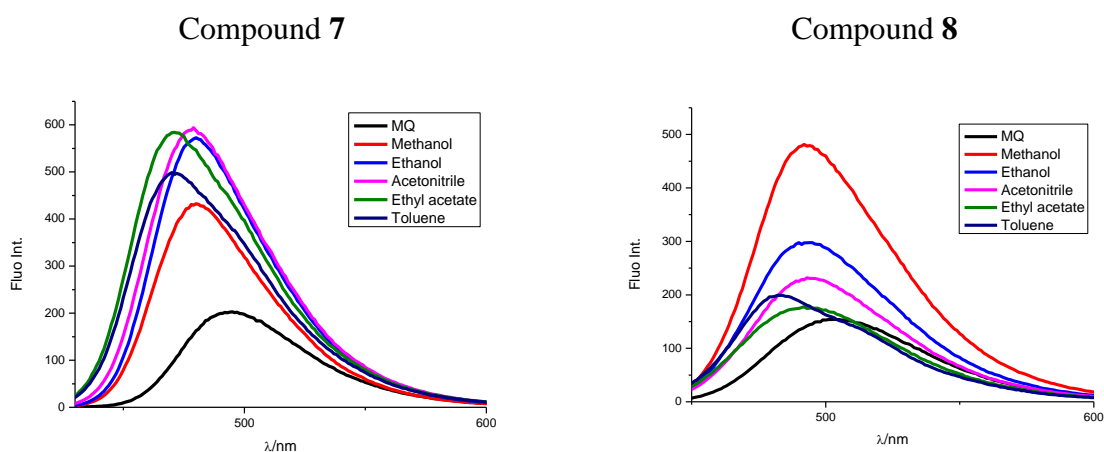


Figure 3. Experimentally measured emission spectra of **7** ($\lambda_{exc} = 420$ nm) and **8** ($\lambda_{exc} = 420$ nm) at concentration 1×10^{-7} mol dm $^{-3}$ in organic solvents of varying polarities

Table 1. Electronic absorption and emission data for all studied compounds

Compound		MQ water	Methanol	Ethanol	Acetonitrile	Ethyl acetate	Toluene
	E_T (30)	63.1	55.4	51.9	45.6	38.1	33.9
4	λ_{abs}/nm	425	423	421	427	425	431
	$\epsilon \times 10^3 / dm^3 mol^{-1} cm^{-1}$	18.9	25.5	27.9	39.4	39.7	35.8
	λ_{emiss}/nm	-	-	-	-	-	-
5	λ_{abs}/nm	410	410	408	406	398	402
	$\epsilon \times 10^3 / dm^3 mol^{-1} cm^{-1}$	21.3	14.4	30.2	6.6	29.7	34.7
	λ_{emiss}/nm	-	-	-	-	-	-
7	λ_{abs}/nm	472	439	438	437	432	455
		443	286	286	286	284	437
		291					314
	$\epsilon \times 10^3 / dm^3 mol^{-1} cm^{-1}$	29.1	40.4	48.15	50.6	50.55	46.25
		37.55	11	12.7	13.9	13.4	47.85
	13.9					5.6	
	λ_{emiss}/nm	495	480	481	479	469	469
8	λ_{abs}/nm	445	419	419	412	403	423
		221	220	220	220		
	$\epsilon \times 10^3 / dm^3 mol^{-1} cm^{-1}$	26.5	17.4	32.7	32.5	25.2	30.8
	45.3	33.7	58.6	57.6			
	λ_{emiss}/nm	506	492	492	494	492	481
11	λ_{abs}/nm	425	418	419	415	414	421
		279	281	280	281	280	407
	$\epsilon \times 10^3 / dm^3 mol^{-1} cm^{-1}$	30.95	37.85	34.4	38.8	36.99	35.3
	4.87	5.0	4.7	5.2	5.2	33.0	
	λ_{emiss}/nm	-	-	-	421	417	-
12	λ_{abs}/nm	465	472	452	429	449	455
		418	345	434	452	428	432
	$\epsilon \times 10^3 / dm^3 mol^{-1} cm^{-1}$	21.6	27	56.1	54.3	49.7	46.1
	37.4	3.3	67.2		65.8	61.9	
	λ_{emiss}/nm	493	479	471	479	417	455

The strongest fluorescence intensity of **7** was demonstrated in ethanol, acetonitrile and ethyl acetate with a slight hypsochromic shift of maxima relative to spectra taken in water (~15 nm). We observed a slight bathochromic shift of emission maxima in methanol, ethanol and acetonitrile relative to spectra taken in toluene and ethyl acetate. Compound **8** showed the bathochromic shift of emission maxima in MQ water when compared to all others solvents (~10 nm). The strongest hyperchromic effect of the intensity has been observed in methanol. The strongest hypochromic effect with the significant decrease of the intensity has been observed in MQ water and ethyl acetate. Acrylonitriles **4–5** did not show any measurable fluorescence intensity in any solvent (Fig. S17), while Schiff bases **11–12** revealed only very low fluorescence intensity (Fig. S17).

2.2.3. Experimental acid-base properties of studied benzimidazole derivatives

To study the possibility of a potential use of the prepared benzimidazoles as optical pH indicators, the influence of their spectroscopic properties relative to changes in the pH conditions was determined through the spectroscopic UV-Vis and fluorescence pH titrations. Aqueous-solution pK_a values are typically used to characterize potential optical pH sensors, as useful parameters to determine precise protonation states of a studied molecule. They can be determined from the obtained spectroscopic data, which rely on the optical determination of the concentrations of the acidic (HA) and basic forms (A^-) through the Henderson–Hasselbalch equation:⁴⁰

$$pH = pK_a + \log \frac{[A^-]}{[HA]}$$

pH dependence of spectral properties was studied by spectroscopic UV-Vis and fluorescence pH titrations. Changing the pH conditions caused the protonation/deprotonation of studied compounds, leading to the reorganization of the electron density within the structural units following the accompanying generation of the excess charge.

Absorption spectra taken at the pH range from 1 to 13 confirmed pronounced spectral changes, thereby confirming the possible use of the studied benzimidazoles as pH optical probes (Fig. 4, Table 2). Spectral properties upon pH titrations for all benzimidazoles are presented in Table 2. Considering the obtained results, the most significant changes are observed in strong acidic media (pH 1) for all studied compounds, especially Schiff bases **11** and **12** which showed almost total decrease of absorbance intensity when compared to spectra taken in neutral (pH 7). At pH 2 we can observe the strong increase of absorption intensity and red shift of maxima for

compound **11** relative to spectra at pH 7. At pH 1, acrylonitriles **4** and **5** showed a significant red shift of absorption maxima as well as strong hypochromic effect of intensity (Fig. 5), while at pH 2, there is a strong hyperchromic effect.

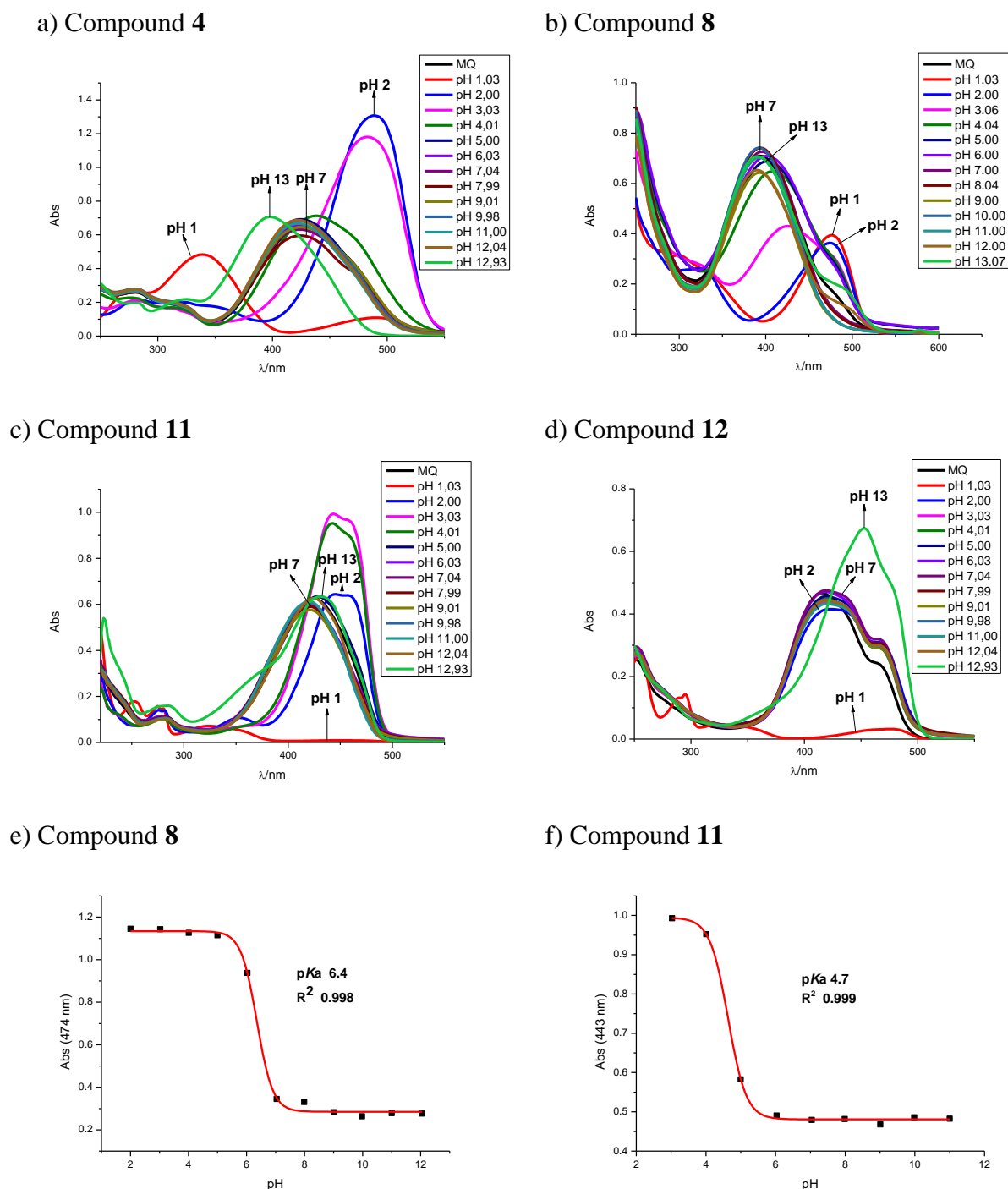


Figure 4. Absorption spectra of studied compounds **4**, **8**, **11** and **12** at different pH values in buffer (a, b, c, d); ratiometric absorption pH titration curve for compounds **8** and **11** from which the pK_a was obtained by using a Boltzmann curve (e, f).

In highly basic condition (pH = 13), unsubstituted acrylonitrile **4** showed hypsochromic shift in comparison to spectra taken at pH 7, while *N*-phenyl and cyano substituted acrylonitrile **5** showed almost the same spectra as at pH 7. Iminocoumarin derivatives **7** and **8** showed bathochromic shift of absorption maxima in acidic condition at pH 1 in comparison to spectra taken at pH 7. For unsubstituted iminocoumarin **7** we observed the hyperchromic shift and for *N*-phenyl and cyano substituted iminocoumarin **8** hypochromic effect of intensity. For both compounds, the spectra taken at pH 13 are almost unchangeable relative to those at pH 7, thereby indicating that no acid-base changes occur under basic conditions.

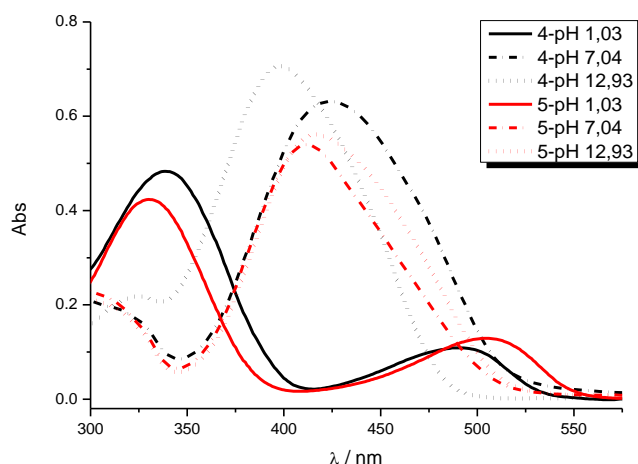


Figure 5. Comparison of absorption pH titration curves for compounds **4** and **5**.

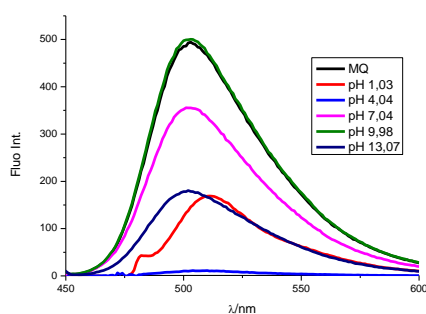
The acid-base features are best described by an ‘apparent’ pK_a value, as opposed to a real thermodynamic pK_a , since pH titrations were not performed under strictly controlled temperature and ionic strength. The pK_a values were determined as the inflection point of a sigmoid Boltzmann curve fitted to the experimental pH titration data (Table 2).

Table 2. pH dependence of absorption for studied compounds in buffered solutions

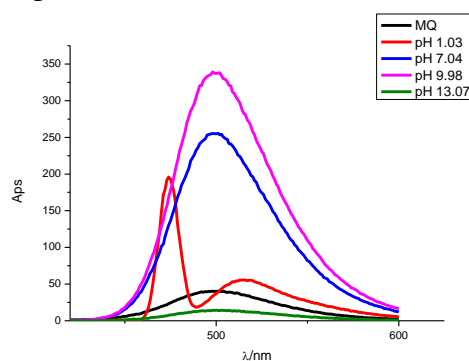
Cpd	λ_{\max} (nm)			$\epsilon \times 10^3$ (dm ³ mol ⁻¹ cm ⁻¹)			$pK_{a(\text{exp})}$
	Acidic	Neutral	Basic	Acidic	Neutral	Basic	
4	340	424	398	24.3	29.9	35.6	3.5
5	330	410	417	21.3	28.3	28.2	1.2 -1.6
7	475	442 472	442 473	74.6	40.9 28.1	40.4 28.0	4.6
8	478	396	391 492	19.9	36.6	35.5 9.1	6.4
11	326	421	432	3.6	29.8	31.7	4.6
12	479	418 467	453	1.8	23.9 16.1	33.7	-0.9

Emission spectra taken at pH values 1, 4, 7, 10 and 13 confirmed pronounced spectral changes for iminocoumarines **7–8**, thereby supporting their potential use as pH optical probes (Fig. 6). Considering the results obtained for **7**, the most significant changes are observed at pH 4 with a total decrease of intensity, in strong acidic media (pH 1) and strong basic media (pH 13), when compared to the spectra taken at pH 7 and in MQ water. At pH ~10, compound **7** showed the fluorescence intensity increase. On the other hand, compound **8** revealed the intensity decrease in strong basic media at pH 13, while in strong acidic media the data showed two emission bands with relatively low fluorescence intensity and slight bathochromic shift of emission maxima. The most significant increase of fluorescence intensity is observed at pH 10. Interestingly, the cyano substituted Schiff base **12** which did not showed significant fluorescence intensity in organic solvents, showed the significant increase of intensity in neutral at pH 7 and in strong basic media at pH 13.

Compound **7**



Compound **8**



Compound **12**

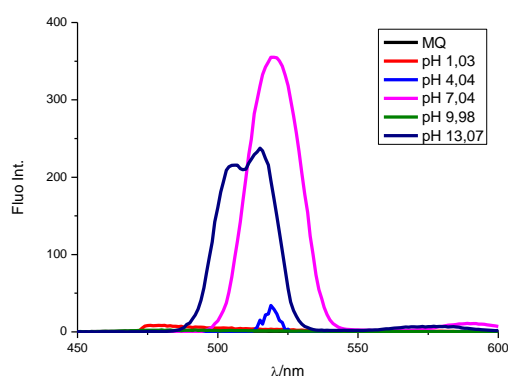


Figure 5. Emission spectra of studied compounds **7**, **8** and **12** at different pH values in buffer taken at the concentration of $1 \times 10^{-7} \text{ mol dm}^{-3}$

2.3. Computational analysis

Computational analysis was used to elucidate predominant protonation forms of each system in solution that are responsible for the observed photophysical property alterations following pH conditions changes. For that purpose, we employed the B3LYP/6-311++G(2df,2pd)//(SMD)/B3LYP/6-31+G(d) model to calculate the matching aqueous phase pK_a values, which are presented in a brief form in Table 3, while a more extensive illustration is given in Figure S3. The obtained data reveal a very good agreement with measurements, in a way that most computed values are found within the acceptable margin of 1 pK_a unit from experiments. The only two exceptions are noted for derivatives **7** and **8**, where computations overestimate the corresponding basicities by 3.6 and 2.4 pK_a units, respectively, an aspect that we will come back to later in the text.

It is interesting to observe that, according to the measured acid-base constants, all molecules are unionized systems under neutral conditions, as evident from their pK_a values for the most basic position that are all found below 7. Starting with the seemingly simplest acrylonitriles **4** and **5**, their most basic sites correspond to the benzimidazole nitrogen, where the calculated values of $pK_a(\mathbf{4}) = 4.7$ and $pK_a(\mathbf{5}) = 2.0$ are well-matched with measured values 3.5 and 1.2, in the same order. Interestingly, both systems are significantly less basic than their parent benzimidazole ($pK_{a,\text{exp}} = 5.6$).⁴¹ In **4**, this is ascribed to the electron accepting ability of the unsaturated acrylo unit, which is in a direct resonance interaction with the basic benzimidazole nitrogen, further furnished by the strong electron accepting nitrile moiety. It appears that a synergic effect of the acrylonitrile unit components overcomes a likely favorable contribution of a strong electron donating diethylamino group, whose typical basicity-enhancing effect can be illustrated by, for example, its ability to improve the basicity of pyridine from 5.2 to 9.7 once it is attached in the *para* position.⁴¹ Still, due to a much distant nature, its positive effect is over dominated by a basicity suppression effect of a more closer acrylonitrile fragment. In **5**, the basicity lowering trend is even more pronounced due to two effects: (i) the direct attachment of an additional cyano moiety onto the benzimidazole core, and (ii) converting the secondary benzimidazole amine into its *N*-phenyl analogue. This is a common feature observed in all six studied derivatives, where the matching benzimidazole nitrogen turns less basic once its neighboring amine is *N*-phenylated, and additional nitrile is inserted onto the benzimidazole skeleton. Both effects represent a typical behavior observed in a large variety of systems; for example, the basicity of *N*-phenylimidazole is lowered from $pK_a = 7.0$ to $pK_a = 5.1$ relative to the parent imidazole,⁴¹ while a strong basicity-diminishing effect of the resonantly coupled nitrile is broadly documented in the literature.^{42, 43} Because of the same reasons, and since its

protonation occurs on already protonated derivatives **4**⁺ and **5**⁺, the basicity of diethylamino group is drastically suppressed, -1.8 in **4** and -2.3 in **5**, which is far from what is typically achieved for this functionality in, let us say, *N,N*-diethylaniline, where it is $pK_{a,\text{exp}} = 6.9$.⁴¹ Lastly, the N–H acidity within the benzimidazole unit in **4** is calculated at $pK_a = 15.3$, thereby also being much lower than in the parent benzimidazole, where it is 12.9 .⁴¹ Nevertheless, all of this suggests that acrylonitrile-based derivatives **4** and **5** could be employed as potential pH probes, yet only for highly acidic media around $\text{pH} \approx 1\text{--}4$, where the corresponding transition from the unionized to monocationic derivatives occurs.

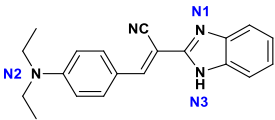
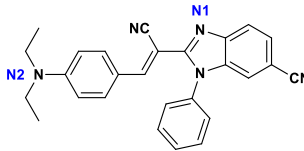
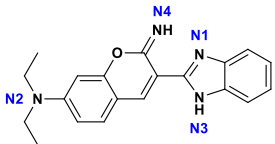
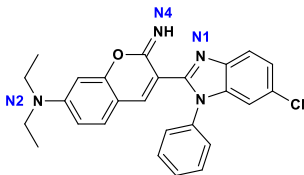
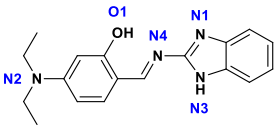
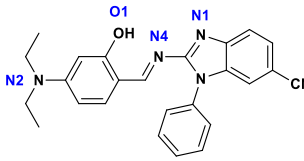
When Schiff base derivatives **11** and **12** are considered, one could expect notably more basic systems, based on the fact that the parent benzenemethanimine (Ph-CH=NH) is already appreciably basic at $pK_a = 7.0$,⁴¹ let alone a likely significant basicity-promoting contribution from the *p*-NEt₂ group. Still, when the aromatic moiety is attached directly to the protonating imine, it results in a drastic lowering of the basicity, where the former moiety depletes the electron density from the imine, thereby reducing its proton accepting ability. As an illustration, the basicity of *N*-phenylbenzenemethanimine (Ph-CH=N-Ph) drops over 4 pK_a units to a value of $pK_a = 2.8$,⁴¹ an effect that is also observed in several guanidines as well.⁴⁴ All of this is nicely evident in **11** and **12**, where the basicity of the Schiff base imine is even preceded by the benzimidazole nitrogen, which retains its basicity around $pK_a \approx 4\text{--}5$ and is identified as the most basic site in both **11** and **12**. In addition, the O–H \cdots N hydrogen bonding with the vicinal phenol, seen in both unionized systems, further contributes to the lower Schiff base imine basicity, through stabilizing the system prior to the protonation. Although the calculated value for the Schiff base imine protonation in **12** ($pK_a = -0.9$) is found in a very good agreement with experiments ($pK_a = -2.0$), such low values bear little significance for the potential applications of systems **11–12** as pH probes in broad areas, due to extreme acidity conditions to which they respond. In contrast, the fact that both **11–12** exchange protonation forms and give modified photophysical responses at $\text{pH} \approx 4\text{--}5$, makes them more appealing for further derivatization over their acrylonitrile analogues. We note in passing that the acidity of phenols in both derivatives and that of benzimidazole in **11** exceeds conditions employed in this work ($pK_a > 14$) and were, therefore, not observed in our experiments.

Values measured for iminocoumarins, $pK_a(\mathbf{7}) = 4.6$ and $pK_a(\mathbf{8}) = 6.4$, illustrate their potential for the application in a large variety of academic and industrial application, since they respond under already moderately acidic conditions, especially the latter. Employing the same computational model as here, our earlier work on a series of similar iminocoumarins revealed excellent agreement between computed and measured pK_a data,²⁵ which leaves it unclear for the

reasons underlying 2.4–3.6 pK_a units discrepancy observed here. Still, more importantly, we are confident that our calculations correctly identified the iminocoumarin moiety as the most basic site in **7–8**, since it is several kcal mol⁻¹ more favorable over benzimidazole for the first protonation. Interestingly, the basicity of both benzimidazole rings is reduced because of a favorable =N–H \cdots N hydrogen bonding with the nearby iminocoumarin that stabilizes neutral benzimidazole and diminishes its basicity, which is established only at pH \approx 0 in both **7–8**.

Lastly, to further confirm the validity of our pK_a calculations and the identification of the relevant protonation states, we have calculated the matching UV-Vis transitions pertaining to different protonation forms that were identified to occur under employed experimental conditions (Figure S4). On the overall, the computed data are found in good agreement with experiments and trends in the position of the measured absorption maxima. For both unionized acrylonitriles **4** and **5**, the most dominant feature is a broad absorption at around 400 nm, which well-matches experiments and confirms the predominance of this form at neutral pH = 7. Because of its *N*-phenyl moiety, **5** does not possess an acidic hydrogen, which is why its bands at pH = 7 and pH = 13 are overlapped (Figure S2), while computations correctly predict a red shift of the absorption maxima for deprotonated **4**⁻ at pH = 13. Analogously, bands computed for monoprotonated **4**⁺ and **5**⁺ confirm the absorption blue shift, while rationalize a large red shift at lowest pH values that appear close to 300 nm, which validates the existence of the protonated diethylamine under very acidic conditions (pH = 1). Furthermore, given the calculated negative pK_a values required to achieve diethylamine protonation, at pH = 1 there is only a few percent of the matching dications in solution, which corroborates a very strong hypochromic effect of their absorption intensity observed experimentally. For iminocoumarins **7** and **8**, computed pK_a values around zero predict the possibility for the existence of the matching dications at lowest pH conditions, while the obtained overlap of their absorption bands with those for monocations, although both correctly red shifted, makes it indistinct to claim their presence. An analogous overlap is observed experimentally for bands at pH = 7 and pH = 13, which is rationalized by the absence of the acidic proton in **7** and, according to our calculations, a very low acidity of the benzimidazole proton in **8** ($pK_a = 17.3$). Schiff bases **11** and **12** are associated with the largest red shift under basic condition, which is well reproduced by our calculations. As with **7**, the significant overlap of bands corresponding to **11**⁻ and **11**²⁻ disallows any certainty in claiming the presence of the latter, although a very low basicity of the benzimidazole proton ($pK_a = 18.2$) suggests only monoanions are present under employed basic conditions. The latter correspond to the phenol deprotonation, being achieved at around $pK_a \approx 14$ in both **11** and **12**.

Table 3. Calculated aqueous-phase pK_a values by the B3LYP/6-311++G(2df,2pd)//(SMD)/B3LYP/6-31+G(d) model. Experimental values determined here are given in square brackets for an easier comparison.

System	State	$pK_a(\text{calc})$	Protonation Reaction	System	State	$pK_a(\text{calc})$	Protonation Reaction	
	4^{2+}				5^{2+}			
	\uparrow	-1.8	$N2 \rightarrow N2^+$		\uparrow	-2.3 [-1.6] _{exp}	$N2 \rightarrow N2^+$	
	4^+				5^+			
	\uparrow	4.7 [3.5] _{exp}	$N1 \rightarrow N1^+$		\uparrow	2.0 [1.2] _{exp}	$N1 \rightarrow N1^+$	
4			5					
	\downarrow	15.3	$N3 \rightarrow N3^-$					
	4^-							
	7^{3+}				8^{3+}			
	\uparrow	-5.9	$N2 \rightarrow N2^+$		\uparrow	-5.4	$N2 \rightarrow N2^+$	
	7^{2+}				8^{2+}			
	\uparrow	0.7	$N1 \rightarrow N1^+$		\uparrow	0.0	$N1 \rightarrow N1^+$	
	7^+				8^+			
\uparrow	8.2 [4.6] _{exp}	$N4 \rightarrow N4^+$	\uparrow	8.8 [6.4] _{exp}	$N4 \rightarrow N4^+$			
7			8					
	\downarrow	17.3	$N3 \rightarrow N3^-$					
	7^-							
	11^{3+}				12^{3+}			
	\uparrow	-10.4	$N2 \rightarrow N2^+$		\uparrow	-11.1	$N2 \rightarrow N2^+$	
	11^{2+}				12^{2+}			
	\uparrow	-1.6	$N4 \rightarrow N4^+$		\uparrow	-2.0 [-0.9] _{exp}	$N4 \rightarrow N4^+$	
	11^+				12^+			
	\uparrow	5.6 [4.6] _{exp}	$N1 \rightarrow N1^+$		\uparrow	4.2	$N1 \rightarrow N1^+$	
11			12					
	\downarrow	14.5	$O1 \rightarrow O1^-$					
	11^-							
	\downarrow	18.2	$N3 \rightarrow N3^-$					
	11^{2-}							

3. Conclusions

We present the design and synthesis of D- π -A benzimidazoles with carefully chosen electron donating and electron accepting substituents to confirm their potential as optical sensors for the pH detection in solutions. These molecules are substituted at the *para* position of phenyl ring with an electron donating *N,N*-diethylamino group and an electron accepting cyano group placed at the benzimidazole nuclei, which is also pH sensitive due to the two imidazole N atoms. To study the influence of the central core on spectroscopic properties, we have prepared two acrylonitrile, two Schiff bases and two iminocoumarin derived benzimidazoles.

The spectroscopic characterization has been carried out with UV-Vis and fluorescence spectroscopies in several organic solvents, as well as in aqueous solution buffers with different pH. Absorption spectra were strongly influenced by the solvent polarity, while the type of the phenyl and benzimidazole substituents, together with the type of central core affected their photophysical features. Their potential application as optical pH sensors was determined by absorption and fluorescence pH titrations, which showed that modified pH conditions exert significantly different responses. This was confirmed by experimentally determined aqueous solution *pK*_a values and further supported by DFT calculations, which achieved good agreement with measurements.

Computational analysis identified predominant protonation forms of each investigated system in solution, which are responsible for the observed changes in the photophysical properties following changes in the pH conditions. The obtained insight revealed that all systems are unionized molecules under neutral conditions, whereas they transit into monocationic derivatives under acidic conditions, which is responsible for modified responses observed in the UV-Vis spectra. The most basic site in both acrylonitrile- and Schiff base-based derivatives is the benzimidazole nitrogen, with all four studied systems being less basic than the parent benzimidazole, due to the employed molecular design dominated by the electron-withdrawing moieties in the nearest vicinity of the basic center. While for the studied acrylonitrile derivatives **4–5** the matching protonation form change occurs under highly acidic conditions (pH \approx 1–4), for Schiff base derivatives **11–12** this is observed within less extreme environments (pH \approx 4–5), which makes them more appealing for practical implementations. Yet, the full potential of our strategy is achieved in the iminocoumarin-based derivatives **7–8**, where the relevant transition from the neutral to the monocation forms is achieved at pH = 4.6 for **7** and pH = 6.4 for **8**, thereby revealing their sensitivity to already mildly acidic conditions.

4. Experimental part

4.1. Chemistry

4.1.1. General methods

All chemicals and solvents were purchased from commercial suppliers. Melting points of prepared compounds were recorded on SMP11 Bibby and were not corrected. NMR spectra were measured in DMSO-*d*₆ solutions using TMS as an internal standard on a Varian Gemini 300 or Varian Gemini 600 spectrophotometer at 300, 400, 600, 100, 110, 151 and 75 MHz. Chemical shifts are reported in parts per million (ppm) relative to TMS. Elemental analyses for carbon, hydrogen and nitrogen were performed on Perkin-Elmer 2400 elemental analyser. Analyses are indicated as symbols of elements, analytical results obtained are within 0.4 % of the theoretical value. All compounds were routinely checked by TLC using Merck silica gel 60F-254 glass plates.

4.1.2. Synthesis

Synthesis of main precursors necessary for the synthesis of targeted benzimidazole derivatives, namely 2-cyanomethylbenzimidazole, 6-cyano-2-cyanomethyl-*N*-phenylbenzimidazole and 2-amino-6-cyano-*N*-phenylbenzimidazole was carried out according to the previously published procedures.⁴⁵

4.1.2.1. General method for preparation of compounds 4–5, 7–8, 11–12

Solution of equimolar amounts of 2-cyanomethylbenzimidazoles 1–2 or 2-amino-benzimidazoles 9–10, corresponding heteroaromatic aldehyde 3 or 6 and few drops of piperidine in absolute ethanol, were refluxed for 2–48 hours. The cooled reaction mixture was filtered and, if necessary, product was purified by column chromatography on SiO₂ using dichloromethane/methanol as eluent.

(E)-2-(1*H*-benzimidazol-2-yl)-3-(4-*N,N*-diethylaminophenyl)acrylonitrile 4

Compound 4 was prepared from 1 (0.10 g, 0.6 mmol) and 3 (0.11 g, 0.6 mmol) in absolute ethanol (2 mL) after refluxing for 3 hours to yield 0.14 g (68 %) of orange powder. m.p 151–156 °C; ¹H NMR (DMSO-*d*₆, 300 MHz): δ/ppm = 12.75 (s, 1H, NH_{benzimidazole}), 8.10 (s, 1H, H_{arom.}), 7.97–7.81 (m, 3H, H_{arom.}), 7.53 (bs, 2H, H_{arom.}), 7.23–7.17 (m, 1H, H_{arom.}), 6.87–6.77 (m, 2H, H_{arom.}), 3.47 (q, 4H, *J* = 6.45 Hz, CH₂), 1.15 (t, 6H, *J* = 6.68 Hz, CH₃); ¹³C NMR (DMSO-*d*₆, 151 MHz): δ/ppm = 150.6, 149.5, 145.9, 144.0, 135.3, 133.5, 132.8, 123.2, 122.3, 119.6, 119.0, 118.4 (2C), 111.8, 111.6, 93.4, 44.4 (2C), 12.9 (2C); Anal. Calcd. for C₂₀H₂₀N₄: C, 75.92; H, 6.37; N, 17.71. Found: C, 75.97; H, 6.46; N, 17.76%.

(E)-2-(6-cyano-*N*-phenylbenzimidazol-2-yl)-3-(4-*N,N*-diethylaminophenyl)acrylonitrile 5

Compound **5** was prepared from **2** (0.10 g, 0.4 mmol) and **3** (0.07 g, 0.4 mmol) in absolute ethanol (2 mL) after refluxing for 2 hours to yield 0.14 g (86 %) of red powder. m.p 210–214 °C; ¹H NMR (DMSO-*d*₆, 300 MHz): δ/ppm = 8.31 (d, 1H, *J* = 0.78 Hz, H_{arom.}), 7.74 (s, 2H, H_{arom.}), 7.70 (s, 1H, H_{arom.}), 7.69–7.57 (m, 6H, H_{arom.}), 7.29 (d, 1H, *J* = 8.47 Hz, H_{arom.}), 6.77 (d, 2H, *J* = 9.09 Hz, H_{arom.}), 3.45 (q, 4H, *J* = 6.89 Hz, H_{arom.}), 1.13 (t, 6H, *J* = 6.97 Hz, H_{arom.}); ¹³C NMR (DMSO-*d*₆, 75 MHz): δ/ppm = 151.7, 151.5, 151.2, 142.2, 140.3, 135.3, 133.2 (2C), 130.7 (2C), 130.3, 128.1 (2C), 127.2, 124.2, 120.1, 119.3, 117.4, 112.2, 111.8, 105.7, 90.1, 44.5 (2C), 12.7 (2C); Anal. Calcd. for C₂₇H₂₃N₅: C, 77.67; H, 5.55; N, 16.77. Found: C, 77.61; H, 5.66; N, 16.73%.

3-(1H-benzo[d]imidazol-2-yl)-N,N-diethyl-2-imino-2H-chromen-7-amine 7

Compound **7** was prepared from **1** (0.05 g, 0.2 mmol) and **6** (0.04 g, 0.2 mmol) in absolute ethanol (2 mL) after refluxing for 4.5 hours to yield 0.05 g (64 %) of orange powder. m.p °C; ¹H NMR (DMSO-*d*₆, 300 MHz): δ/ppm = 12.26 (s, 1H, NH_{benzimidazole}), 8.92 (s, 1H, NH), 7.71 (d, 1H, *J* = 8.97 Hz, H_{arom.}), 7.61 (bs, 2H, H_{arom.}), 7.19–7.13 (m, 2H, H_{arom.}), 6.83 (dd, 1H, *J*₁ = 2.36 Hz, *J*₂ = 8.97 Hz, H_{arom.}), 6.66 (d, 1H, *J* = 2.18 Hz, H_{arom.}), 5.75 (s, 1H, H_{arom.}), 3.50 (q, 4H, *J* = 6.99 Hz, CH₂), 1.16 (t, 6H, *J* = 6.98 Hz, CH₃); ¹³C NMR (DMSO-*d*₆, 151 MHz): δ/ppm = 160.2, 156.5, 151.6, 147.2, 143.0, 130.8, 121.8, 110.0, 108.1, 107.9, 96.2, 44.3 (2C), 12.3 (2C); Anal. Calcd. for C₂₀H₂₀N₄O: C, 72.27; H, 6.06; N, 16.86. Found: C, 72.19; H, 5.98; N, 16.84%.

2-(7-(diethylamino)-2-imino-2H-chromen-3-yl)-1-phenyl-1H-benzo[d]imidazole-6-carbonitrile 8

Compound **8** was prepared from **2** (0.05 g, 0.2 mmol) and **6** (0.04 g, 0.2 mmol) in absolute ethanol (2 mL) after refluxing for 4.5 hours to yield 0.05 g (64 %) of orange powder. m.p 238–241 °C; ¹H NMR (DMSO-*d*₆, 400 MHz): δ/ppm = 8.39–8.33 (m, 1H, H_{arom.}), 7.76 (d, 1H, *J* = 9.97 Hz, H_{arom.}), 7.68 (d, 1H, *J* = 8.28 Hz, H_{arom.}), 7.64–7.44 (m, 5H, H_{arom.}), 7.34 (bs, 1H, H_{arom.}), 7.04–6.89 (m, 1H, H_{arom.}), 6.53–6.46 (m, 1H, H_{arom.}), 6.38–6.25 (m, 1H, H_{arom.}), 3.40 (q, 4H, *J* = 6.85 Hz, CH₂), 1.10 (t, 6H, *J* = 6.92 Hz, CH₃); ¹³C NMR (DMSO-*d*₆, 110 MHz): δ/ppm = 160.9, 153.0, 152.6, 144.9, 142.3, 140.4, 135.4, 130.7, 130.2, 129.1, 128.0, 126.9, 124.6, 123.9, 120.2, 118.2, 112.0, 108.5, 108.0, 105.5, 105.3, 96.6, 87.2, 44.6 (2C). 31.2, 12.9; Anal. Calcd. for C₂₇H₂₃N₅O: C, 74.81; H, 5.35; N, 16.16. Found: C, 74.75; H, 5.30; N, 16.09%.

(E)-2-(((1H-benzo[d]imidazol-2-yl)imino)methyl)-5-(diethylamino)phenol 11

Compound **11** was prepared from **9** (0.25 g, 1.9 mmol) and **6** (0.36 g, 1.9 mmol) in absolute ethanol (10 mL) after refluxing for 48 h to yield 0.13 g (22 %) of green powder. m.p. 122–125°C; ¹H NMR (DMSO-*d*₆, 600 MHz): δ/ppm = 12.83 (s, 1H, NH_{benzimidazole}), 12.36 (s, 1H, OH), 9.31 (s, 1H, H_{arom.}), 7.50 (s, 1H, H_{arom.}), 7.48 (s, 1H, H_{arom.}), 7.38 (bs, 1H, H_{arom.}), 7.14–7.10 (m, 2H,

H_{arom.}), 6.39 (dd, 1H, $J_1 = 2.07$ Hz, $J_2 = 8.86$ Hz, H_{arom.}), 6.14 (d, 1H, $J = 1.99$ Hz, H_{arom.}), 3.43 (q, 4H, $J = 6.98$ Hz, CH₂), 1.14 (t, 6H, $J = 6.97$ Hz, CH₃); ¹³C NMR (DMSO-*d*₆, 75 MHz): δ /ppm = 164.6, 164.0, 155.2, 153.1, 135.7, 121.9 (2C), 108.8, 105.3, 97.2, 44.6 (2C), 13.0 (2C); Anal. Calcd. for C₁₈H₂₀N₄O: C, 70.11; H, 6.54; N, 18.17. Found: C, 70.16; H, 6.62; N, 18.26%.

(E)-2-((4-(diethylamino)-2-hydroxybenzylidene)amino)-1-phenyl-1H-benzo[d]imidazole-6-carbonitrile **12**

Compound **12** was prepared from **10** (0.20 g, 0.9 mmol) and **6** (0.16 g, 0.9 mmol) in absolute ethanol (10 mL) after refluxing for 48 h to yield 0.23 g (66 %) of yellow powder. m.p. 111–114 °C; ¹H NMR (400 MHz, DMSO-*d*₆) (δ /ppm): 12.28 (bs, 1H, OH), 9.37 (s, 1H, H_{arom.}), 8.13–8.11 (m, 1H, H_{arom.}), 7.68–7.64 (m, 2H, H_{arom.}), 7.61–7.59 (m, 3H, H_{arom.}), 7.56 (dd, 1H, $J_1 = 8.28$ Hz, $J_2 = 1.56$ Hz, H_{arom.}), 7.51 (d, 1H, $J = 9.09$ Hz, H_{arom.}), 7.35 (d, 1H, $J = 8.37$ Hz, H_{arom.}), 6.40 (dd, 1H, $J_1 = 9.08$ Hz, $J_2 = 2.40$ Hz, H_{arom.}), 6.04 (d, 1H, $J = 2.28$ Hz, H_{arom.}), 3.44–3.39 (m, 1H, CH₂), 1.11 (t, 6H, $J = 7.01$ Hz, CH₃); ¹³C NMR (100 MHz, DMSO-*d*₆) (δ /ppm): 165.8, 164.4, 156.8, 154.0, 142.0, 138.6, 136.4, 134.7, 130.3, 129.3, 127.8, 126.2, 122.9, 120.4, 111.5, 109.1, 105.9, 105.0, 96.9, 44.7 (2C), 13.0 (2C); Anal. Calcd. for C₂₅H₂₃N₅O: C, 73.33; H, 5.66; N, 17.10. Found: C, 73.36; H, 5.69; N, 17.15%.

4.2. Spectroscopic characterization

Absorption spectra were taken in different organic solvents with various polarity parameters⁴⁶ at the same concentration and at room temperature, using a Varian Cary 50 spectrophotometer in double-beam mode, where the employed water was additionally purified using a Millipore Milli-Q lab water system and denoted as MQ-water throughout the text. The wavelength range covered was 200–650 nm. Quartz cells of 1 cm path length were used throughout and the absorbance values were recorded at 0.1 nm. In order to study the effect of pH on the spectroscopic properties of studied benzimidazoles, UV-Vis spectra were recorded in universal buffer solutions covering the pH range 1–13. Solutions of 0.1 mol dm⁻³ hydrochloric acid and 0.1 mol dm⁻³ sodium hydroxide were used as terminal acidic and basic points in the titration experiments with 2×10^{-5} mol dm⁻³ solutions of compounds for the absorbance measurements. Fluorescence measurements were recorded on Varian Cary Eclipse fluorescence spectrophotometer in quartz cells of 1 cm path length. Excitation maxima were determined from absorption spectra in the range of 200–500 nm. Emission spectra were recorded in the range from 400–600 nm and were corrected for the effects of time- and wavelength-dependent light-source fluctuations using a standard of rhodamine 101.

4.3. Computational analysis

All molecular geometries were optimized with the efficient B3LYP/6-31+G(d) model, providing a good compromise between accuracy and feasibility of the approach. The obtained electronic energies were supplemented with thermal corrections, extracted from the matching unscaled frequency calculations, so that all values reported here correspond to free energies at room temperature and normal pressure. Gas-phase energies were further refined with single-point calculations through a more flexible 6-311++G(2df,2pd) basis set. The effect of the solvent environment was accounted through the SMD polarisable continuum model with all parameters for pure water, yielding the B3LYP/6-311++G(2df,2pd)//(SMD)/B3LYP/6-31+G(d) model employed here. Such a computational setup choice was facilitated by its success in reproducing kinetic and thermodynamic data for a range of organic^{47,48} and biochemical⁴⁹ processes, and in evaluating pK_a values for similar organic derivatives.^{13,37,50} pK_a values were obtained in absolute fashion utilizing the exact gas-phase free energy of a proton, $G^\circ(\text{H}^+) = 6.28 \text{ kcal mol}^{-1}$, and an experimental aqueous-phase solvation free energy of a proton,⁵¹ $\Delta G_{\text{SOLV}}(\text{H}^+) = -265.9 \text{ kcal mol}^{-1}$, to match the value employed by Truhlar and et al.⁵² in parameterizing their implicit SMD model. The latter value includes the free energy contribution of $-1.89 \text{ kcal mol}^{-1}$ required to move from a gas-phase pressure of 1 atm to a liquid-phase concentration of 1 M. UV-Vis electronic transitions were obtained by the (SMD)/CAM-B3LYP/6-31+G(d) single-point calculations employing the TD-DFT approach and considering 32 lowest singlet electronic excitations. All calculations were performed with using the Gaussian 16 suite of programs.⁵³

5. Acknowledgments

This work benefited from the financial support of the Croatian Science Foundation through the grant numbers IP-2020-02-8090 and IP-2018-02-4379. R.V. wishes to thank the Zagreb University Computing Centre (SRCE) for granting computational resources on the ISABELLA cluster.

6. Declaration of Competing Interest

The authors declare that they have no known competing financial interests or personal relationships that could have appeared to influence the work reported in this paper.

7. Appendix A. Supplementary material

Figure S1: Experimentally measured UV–Vis spectra of **5**, **7** and **11** at concentration 2×10^{-5} mol dm^{-3} in organic solvents of varying polarities; compared absorption spectra of all studied compounds in ethanol, ethyl acetate and MQ water. Figure S2: Experimentally measured absorption spectra of **5** and **7** at different pH values. Figure S3: Calculated aqueous-phase pK_a values. Figure S4: Calculated aqueous-phase UV-Vis spectra for different protonation forms of studied systems. Figures S5–S16: NMR spectra of studied compounds. Figure S17: Experimentally measured emission spectra of **4**, **5**, **11** and **12** at concentration 1×10^{-7} mol dm^{-3} in organic solvents of varying polarities.

References

1. E. Horak, R. Vianello, I.M. Steinberg, Optical Sensing (Nano)Materials Based on Benzimidazole Derivatives, Benzimidazole and its Derivatives, IntechOpen, 2019, <https://dx.doi.org/10.5772/intechopen.85643>.
2. J. Kulhanek, F. Bures, O. Pytela, T. Mikysek, J. Ludvik, Imidazole as a Donor/Acceptor Unit in Charge-Transfer Chromophores with Extended π -Linkers, Chem. Asian J. 6 (2011) 1604–1612, <https://doi.org/10.1002/asia.201100097>.
3. G. Yadav, S. Ganguly, Structure activity relationship (SAR) study of benzimidazole scaffold for different biological activities: A mini-review, Eur. J. Med. Chem. 97 (2015) 419–443, <https://doi.org/10.1016/j.ejmech.2014.11.053>.
4. W. Akhtar, M. Faraz Khan, G. Verma, M. Shaquiquzzaman, M.A. Rizvi, S.H. Mehdi, M. Akhter, M. Mumtaz Alam, Therapeutic evolution of benzimidazole derivatives in the last quinquennial period, Eur. J. Med. Chem. 126 (2017) 705–753, <https://doi.org/10.1016/j.ejmech.2016.12.010>.
5. P. Molina, A. Tarraga, F. Oton, Imidazole derivatives: A comprehensive survey of their recognition properties, Org. Biomol. Chem. 10 (2012) 1711–1724, <https://doi.org/10.1039/C2OB06808G>.
6. S. Achelle, J. Rodríguez-López, F. Bureš, F. Robin-le Guen, Tuning the Photophysical Properties of Push-Pull Azaheterocyclic Chromophores by Protonation: A Brief Overview of a French-Spanish-Czech Project, Chem. Rec. 20 (2019) 440–445, <https://doi.org/10.1002/tcr.201900064>.
7. F. Bureš, Fundamental aspects of property tuning in push–pull molecules, RSC Adv. 4 (2014) 58826–58851, <https://doi.org/10.1039/C4RA11264D>.

-
8. M. Klikar, P. Solanke, J. Tydlitát, F. Bureš, Alphabet-Inspired Design of (Hetero)Aromatic Push-Pull Chromophores, *Chem. Rec.* 16 (2016) 1886–1905, <https://dx.doi.org/10.1002/tcr.201600032>.
9. M.Y. Lai, C.H. Chen, W.S. Huang, J.T. Lin, T.H. Ke, L.Y. Chen, M.H. Tsai, C.C. Wu, Benzimidazole/Amine-Based Compounds Capable of Ambipolar Transport for Application in Single-Layer Blue-Emitting OLEDs and as Hosts for Phosphorescent Emitters, *Angew. Chem. Int. Edit.* 47 (2008) 581–585, <https://doi.org/10.1002/anie.200704113>.
10. S. Manoharan, S. Anandan, Cyanovinyl substituted benzimidazole based (D- π -A) organic dyes for fabrication of dye sensitized solar cells, *Dyes Pigm.* 105 (2014) 223–231, <https://doi.org/10.1016/j.dyepig.2014.02.010>.
11. G.M. Saltan, H. Dincalp, M. Kiran, C. Zafer, S.C. Erbas, Novel organic dyes based on phenyl-substituted benzimidazole for dye sensitized solar cells, *Mater. Chem. Phys.* 163 (2015) 387–393, <https://doi.org/10.1039/C4TA02639J>.
12. I.O. de Souza, C.M.L. Schrekker, W. Lopes, R.V.A. Orru, M. Hranjec, N. Perin, M. Machado, L.F. Oliveira, R.K. Donato, V. Stefani et al., Bifunctional Fluorescent Benzimidazo[1,2-*a*]quinolines for *Candida* spp. Biofilm Detection and Biocidal Activity. *J. Photochem. Photobiol. B, Biol.* 163 (2016) 319–326, <https://doi.org/10.1016/j.jphotobiol.2016.08.037>.
13. M. Hranjec, E. Horak, D. Babić, S. Plavljanin, Z. Srdović, I.M. Steinberg, R. Vianello, N. Perin, Fluorescent benzimidazo[1,2-*a*]quinolines: Synthesis, spectroscopic and computational studies of protonation equilibria and metal ion sensitivity, *New J. Chem.* 41 (2017) 358–371, <https://doi.org/10.1039/C6NJ02268E>.
14. K. Tagaki, K. Kusafuka, Y. Ito, K. Yamauchi, K. Ito, R. Fukuda, M. Ehara, Synthesis and Optical Properties of Imidazole- and Benzimidazole-Based Fused π -Conjugated Compounds: Influence of Substituent, Counteranion, and π -Conjugated System, *J. Org. Chem.* 80 (2015) 7172–7183, <https://doi.org/10.1021/acs.joc.5b01028>.
15. H. Li, L. Cai, Z. Chen, Coumarin-derived fluorescent chemosensors, *Advances in Chemical Sensors*, Wang W (Ed.) InTech; 2011. pp. 121–150.
16. L. Xie, Y. Chen, W. Wu, H. Guo, J. Zhao, X. Yu, Fluorescent coumarin derivatives with large Stokes shift, dual emission and solid state luminescent properties: An experimental and theoretical study, *Dyes Pigm.* 92 (2012) 1361–1369, <https://doi.org/10.1016/j.dyepig.2011.09.023>.
17. G. Zhang, H. Zheng, G. Liu, P. Wang, R. Xiang, Synthesis and application of a multifunctional fluorescent polymer based on coumarin, *Bioresources* 11 (2016) 373–384, <https://doi.org/10.15376/biores.11.1.373-384>.
18. G. Zhang, H. Zheng, M. Guo, L. Du, G. Liu, P. Wang, Synthesis of polymeric fluorescent brightener based on coumarin and its performances on paper as light stabilizer, fluorescent

brightener and surface sizing agent, *Appl. Surf. Sci.* 367 (2016) 167–173, <https://doi.org/10.1016/j.apsusc.2016.01.110>.

19. P. Wlodarczyk, S. Komarneni, R. Roy, W.B. White, Enhanced fluorescence of coumarin laser dye in the restricted geometry of a porous nanocomposite, *J. Mater. Chem.* 6 (1996) 1967–1969, <https://doi.org/10.1039/JM9960601967>.

20. R. Sánchez-de-Armas, M.Á. San Miguel, J. Oviedo, J.F. Sanz, Coumarin derivatives for dye sensitized solar cells: a TD-DFT study, *Phys. Chem. Chem. Phys.* 14 (2012) 225–233, <https://doi.org/10.1039/C1CP22058F>.

21. B.D. Wagner, The use of coumarins as environmentally-sensitive fluorescent probes of heterogeneous inclusion systems, *Molecules* 14 (2009) 210–237, <https://doi.org/10.3390/molecules14010210>.

22. A. Shabbir, T. Jang, G. Lee, Y. Pang, Intramolecular charge transfer of coumarin dyes confined in methanol-in-oil reverse micelles, *J. Mol. Liq.* 346 (2022), <https://doi.org/10.1021/la025881x>.

23. H. Xu, Y. Bu, J. Wang, M. Qu, J. Zhang, X. Zhu, G. Liu, Z. Wu, G. Chen, H. Zhou, A convenient fluorescent probe for monitoring lysosomal pH change and imaging mitophagy in living cells, *Sens. Actuators B Chem.* 330 (2021), <https://doi.org/10.1039/C7CC00752C>.

24. A.A. Bhagwat, K.C. Avhad, D.S. Patil, S. Nagaiyan, Design and synthesis of coumarin-imidazole hybrid chromophores: solvatochromism, acidochromism and non-linear optical properties, *Photochem. Photobiol.* 95 (2018) 740–754, <https://doi.org/10.1111/php.13024>.

25. I. Boček, M. Hranjec, R. Vianello, Imidazo[4,5-b]pyridine derived iminocoumarins as potential pH probes: Synthesis, spectroscopic and computational studies of their protonation equilibria, *J. Mol. Liq.* 355 (2022) 118982, <https://doi.org/10.1016/j.molliq.2022.118982>.

26. K. C. Avhad, D. S. Patil, Y. K. C. Gawale, M. C. Subramaniyan Sreenath, I. H. Joe, N. Sekar, Large Stokes Shifted Far-Red to NIR-Emitting D- π -A Coumarins: Combined Synthesis, Experimental, and Computational Investigation of Spectroscopic and Non-Linear Optical Properties, *ChemistrySelect* 3(16) (2018) 4393–4405, <https://doi.org/10.1002/slct.201800063>.

27. W.L. Qin, S. Long, M. Panunzio, S. Biondi, Schiff bases: a short survey on an evergreen chemistry tool, *Molecules* 18 (2013) 12264–12289, <https://doi.org/10.3390/molecules181012264>.

28. A. Kajal, S. Bala, S. Kamboj, N. Sharma, V. Saini, Schiff bases: a versatile pharmacophore, *J. Catal.* 2013 (2013) 893512, <https://doi.org/10.1155/2013/893512>.

29. Q. Feng, Y. Li, L. Wang, C. Li, J. Wang, Y. Liu, et al., Multiple-color aggregation-induced emission (AIE) molecules as chemodosimeters for pH sensing, *Chem. Commun.* 52 (2016) 3123–3126, <https://doi.org/10.1039/C5CC10423H>.

-
30. J. Aljourani, K. Raeissi, M.A. Golozar, Benzimidazole and its derivatives as corrosion inhibitors for mild steel in 1M HCl solution, *Corros. Sci.* 51 (2009) 1836–1843, <https://doi.org/10.1016/j.corsci.2009.05.011>.
31. D. Udhayakumari, V. Inbaraj, A Review on Schiff Base Fluorescent Chemosensors for Cell Imaging Applications, *J. Fluoresc.* 30 (2020) 1203–1223, <https://doi.org/10.1007/s10895-020-02570-7>.
32. H. Tian, X. Qiao, Z.L. Zhang, C.Z. Xie, Q.Z. Li, J.Y. Xu, A high performance 2-hydroxynaphthalene Schiff base fluorescent chemosensor for Al³⁺ and its applications in imaging of living cells and zebrafish in vivo, *Spectrochim. Acta A Mol. Biomol. Spectrosc.* 15 (2019) 31–38, <https://doi.org/10.1016/j.saa.2018.08.063>.
33. V.K. Gupta, A.K. Singh, M.R. Ganjali, P. Norouzi, F. Faridbod, N. Mergu, Comparative study of colorimetric sensors based on newly synthesized Schiff bases, *Sens. Actuators B-Chem.* 182 (2013) 642–651, <https://dx.doi.org/10.1016/j.snb.2013.03.062>.
34. W. Al Zoubi, N. Al Mohanna, Membrane sensors based on Schiff bases as chelating ionophores –A review, *Spectrochim. Acta, Part A* 132 (2014) 854–870, <https://doi.org/10.1016/j.saa.2014.04.176>.
35. E. Horak, P. Kassal, M. Hranjec, I.M. Steinberg, Benzimidazole functionalised Schiff bases: novel pH sensitive fluorescence turn-on chromoionophores for ion-selective optodes. *Sens. Actuators. B Chem.* 258 (2018) 415–423, <https://doi.org/10.1016/j.snb.2017.11.121>.
36. E. Horak, R. Vianello, M. Hranjec, I.M. Steinberg, Colourimetric and fluorimetric metal ion chemosensor based on a benzimidazole functionalised Schiff base, *Supramol. Chem.* 30 (2018) 891–900, <https://doi.org/10.1080/10610278.2018.1436708>.
37. E. Horak, R. Vianello, M. Hranjec, S. Krištafor, G. Karminski Zamola, I. Murković Steinberg. Benzimidazole acrylonitriles as multifunctional push-pull chromophores: spectral characterisation, protonation equilibria and nanoaggregation in aqueous solutions. *Spectrochim. Acta A Mol. Biomol. Spectrosc.* 178 (2017) 225–233, <https://doi.org/10.1016/j.saa.2017.02.011>.
38. O. U. Tan, M. Zengin, Insights into the chemistry and therapeutic potential of acrylonitrile derivatives, *Arch. Pharm.* 355 (2021) e202100383, <https://doi.org/10.1002/ardp.202100383>.
39. E. Horak, M. Hranjec, R. Vianello, I. Steinberg, Reversible pH switchable aggregation-induced emission of self-assembled benzimidazole-based acrylonitrile dye in aqueous solution, *Dyes and pigments* 142 (2017) 108–115 doi: 10.1016/j.dyepig.2017.03.021.
40. A. P. Demchenko, Introduction to fluorescence sensing, *Anal. Bioanal. Chem.* 395 (2009) 1195–1196.

-
41. S. Tshepelevitsh, A. Kütt, M. Lõkov, I. Kaljurand, J. Saame, A. Heering, P. Plieger, R. Vianello, I. Leito, On the Basicity of Organic Bases in Different Media, *E. J. Org. Chem.* 2019 (2019) 6735–6748, <https://doi.org/10.1002/ejoc.201900956>.
42. R. Vianello, Z.B. Maksić, High acidity of polycyano azatriquinanes - theoretical prediction by the DFT calculations, *Tetrahedron Lett.* 46 (2005) 3711–3713, <https://doi.org/10.1016/j.tetlet.2005.03.142>.
43. R. Vianello, Z.B. Maksić, The Acidity of Brønsted CH Acids in DMSO – The Extreme Acidity of Nonacyanocyclononatetraene, *E. J. Org. Chem.* 2004, 5003–5010, <https://doi.org/10.1002/ejoc.200400531>.
44. M. Lõkov, S. Tshepelevitsh, A. Heering, P. G. Plieger, R. Vianello, I. Leito, On the Basicity of Conjugated Nitrogen Heterocycles in Different Media, *E. J. Org. Chem.* 2017 (2017), 4475–4489, <https://doi.org/10.1002/ejoc.201700749>.
45. A. Beč, L. Hok, L. Persoons, E. Vanstreels, D. Daelemans, R. Vianello, M. Hranjec, Synthesis, Computational Analysis, and Antiproliferative Activity of Novel Benzimidazole Acrylonitriles as Tubulin Polymerization Inhibitors: Part 2, *Pharmaceuticals* 14 (2021) 1052, <https://doi.org/10.3390/ph14101052>.
46. J. P. Cerón-Carrasco, D. Jacquemin, C. Laurence, A. Planchat, C. Reichardt, K. Sraïdi, Solvent polarity scales: determination of new $E_T(30)$ values for 84 organic solvents, *J. Phys. Org. Chem.* 27 (2014) 512–518, <https://doi.org/10.1002/poc.3293>.
47. M. Toma, L. Božičević, J. Lapić, S. Đaković, D. Šakić, T. Tandarić, R. Vianello, V. Vrček, Transacylation in Ferrocenoyl-Purines. NMR and Computational Study of the Isomerization Mechanism, *J. Org. Chem.* 84 (2019) 12471–12480, <https://doi.org/10.1021/acs.joc.9b01944>.
48. A. Alizadeh, A. Bagherinejad, J. Kayanian, R. Vianello, An experimental and computational study of new spiro-barbituric acid pyrazoline scaffolds: restricted rotation vs. annular tautomerism, *New J. Chem.* 46 (2022) 7242–7252, <https://doi.org/10.1039/D1NJ06208E>.
49. T. Tandarić, R. Vianello, Computational Insight into the Mechanism of the Irreversible Inhibition of Monoamine Oxidase Enzymes by the Antiparkinsonian Propargylamine Inhibitors Rasagiline and Selegiline, *ACS Chem. Neurosci.* 10 (2019) 3532–3542, <https://doi.org/10.1021/acschemneuro.9b00147>.
50. N. Perin, D. Babić, P. Kassal, A. Čikoš, M. Hranjec, R. Vianello, Spectroscopic and Computational Study of the Protonation Equilibria of Amino-Substituted benzo[*b*]thieno[2,3-*b*]pyrido[1,2-*a*]benzimidazoles as Novel pH-Sensing Materials, *Chemosens.* 10 (2022) 21, <https://doi.org/10.3390/chemosensors10010021>.
51. M.D. Tissandier, K.A. Cowen, W.Y. Feng, E. Gundlach, M.H. Cohen, A.D. Earhart, J.V. Coe, T.R. Tuttle, The Proton's Absolute Aqueous Enthalpy and Gibbs Free Energy of Solvation from

Cluster-Ion Solvation Dana, J. Phys. Chem. A, 102 (1998) 7787–7794, <https://doi.org/10.1021/jp982638r>.

52. A.V. Marenich, C.J. Cramer, D.G. Truhlar, Universal Solvation Model Based on Solute Electron Density and on a Continuum Model of the Solvent Defined by the Bulk Dielectric Constant and Atomic Surface Tensions, J. Phys. Chem. B 113 (2009) 6378–6396, <https://doi.org/10.1021/jp810292n>.

53. Gaussian 16, Revision C.01, M.J. Frisch, G.W. Trucks, H.B. Schlegel, G.E. Scuseria, M.A. Robb, J.R. Cheeseman, G. Scalmani, V. Barone, G.A. Petersson, H. Nakatsuji, X. Li, M. Caricato, A.V. Marenich, J. Bloino, B.G. Janesko, R. Gomperts, B. Mennucci, H.P. Hratchian, J.V. Ortiz, A.F. Izmaylov, J.L. Sonnenberg, D. Williams-Young, F. Ding, F. Lipparini, F. Egidi, J. Goings, B. Peng, A. Petrone, T. Henderson, D. Ranasinghe, V.G. Zakrzewski, J. Gao, N. Rega, G. Zheng, W. Liang, M. Hada, M. Ehara, K. Toyota, R. Fukuda, J. Hasegawa, M. Ishida, T. Nakajima, Y. Honda, O. Kitao, H. Nakai, T. Vreven, K. Throssell, J.A. Montgomery, J.E. Peralta, F. Ogliaro, M.J. Bearpark, J.J. Heyd, E.N. Brothers, K.N. Kudin, V.N. Staroverov, T.A. Keith, R. Kobayashi, J. Normand, K. Raghavachari, A.P. Rendell, J.C. Burant, S.S. Iyengar, J. Tomasi, M. Cossi, J.M. Millam, M. Klene, C. Adamo, R. Cammi, J.W. Ochterski, R.L. Martin, K. Morokuma, O. Farkas, J.B. Foresman, D.J. Fox, Gaussian, Inc., Wallingford CT, 2016.